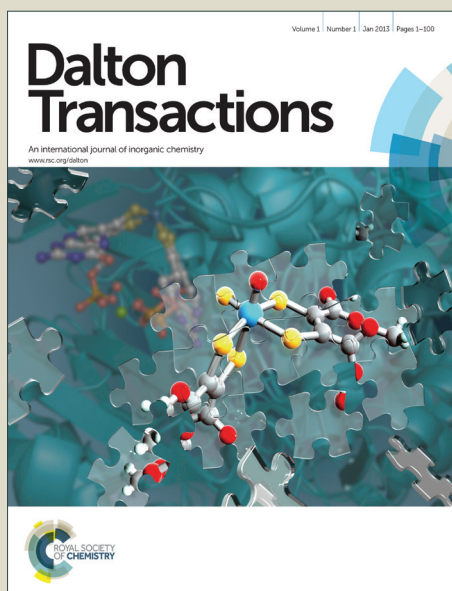


# Dalton Transactions

Accepted Manuscript

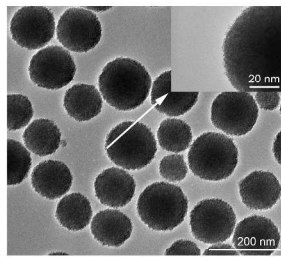


This is an *Accepted Manuscript*, which has been through the Royal Society of Chemistry peer review process and has been accepted for publication.

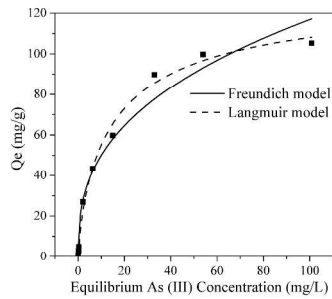
*Accepted Manuscripts* are published online shortly after acceptance, before technical editing, formatting and proof reading. Using this free service, authors can make their results available to the community, in citable form, before we publish the edited article. We will replace this *Accepted Manuscript* with the edited and formatted *Advance Article* as soon as it is available.

You can find more information about *Accepted Manuscripts* in the [Information for Authors](#).

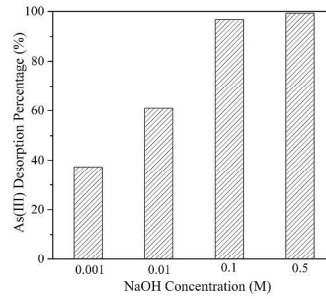
Please note that technical editing may introduce minor changes to the text and/or graphics, which may alter content. The journal's standard [Terms & Conditions](#) and the [Ethical guidelines](#) still apply. In no event shall the Royal Society of Chemistry be held responsible for any errors or omissions in this *Accepted Manuscript* or any consequences arising from the use of any information it contains.



**SnO<sub>2</sub> Nanosphere**



**Favorable Adsorption**



**Easy Desorption**

Graphical Abstract  
454x152mm (300 x 300 DPI)



Journal Name

ARTICLE

## Synthesis of tin oxide nanospheres under ambient conditions and their strong adsorption of As(III) from water

Received 00th January 20xx,  
Accepted 00th January 20xx

DOI: 10.1039/x0xx00000x

www.rsc.org/

Ge Zhang,<sup>a,†</sup> Wuzhu Sun,<sup>a,†</sup> Lingmei Liu,<sup>a</sup> Weiyi Yang,<sup>a</sup> Zhengchao Xu,<sup>b</sup> Qi Li<sup>a,\*</sup> and Jian Ku Shang<sup>c</sup>

The development of highly efficient As(III) adsorbents is critical to largely simplify the arsenic treatment process and lower its cost. For the first time, SnO<sub>2</sub> nanospheres were demonstrated to possess a highly efficient As(III) adsorption capability from water at near neutral pH environment as predicted by the material criterion for the selection of highly efficient arsenic adsorbents we recently developed. These SnO<sub>2</sub> nanospheres were synthesized by a simple and cost-effective hydrolysis process with the assistance of ethyl acetate under ambient conditions, which had a good dispersity, a narrow size distribution, a relatively large specific surface area, and a porous structure. A fast As(III) adsorption was observed in the kinetics study on these SnO<sub>2</sub> nanospheres, and their Langmuir adsorption capacity was determined at ~ 112.7 mg g<sup>-1</sup> at pH ~ 7. The As(III) adsorption mechanism on SnO<sub>2</sub> nanospheres were examined by both macroscopic and microscopic techniques, which demonstrated that it followed the inner-sphere complex model. These SnO<sub>2</sub> nanospheres demonstrated effective As(III) adsorption even with exceptionally high concentrations of co-existing ions, and a good regeneration capability by washing with NaOH solution.

### Introduction

Arsenic is one of the highly toxic contaminants commonly-found in natural water bodies, which is widely spread in many regions of the world, including Bangladesh, China, USA, Chile, and so on.<sup>1</sup> It had been classified as a carcinogen by World Health Organization (WHO), and long-term exposure to arsenic contaminated water could induce a lot of health problems, including cancers of skin, liver, lung, and bladder, skin lesions, cardiovascular disease, neurotoxicity, and diabetes.<sup>2</sup> To reduce its health risk to human beings, its recommended maximum contaminant level (MCL) in drinking water was 10 µg L<sup>-1</sup>.<sup>3</sup> To remove arsenic contamination from water, various technologies have been developed, including ion exchange, reverse osmosis, membrane filtration, coagulation/filtration and adsorption.<sup>2</sup> Among these technologies, the adsorption is believed to be the simplest and most cost-effective approach, especially for arsenic removal from water with relatively low arsenic concentration as that in the natural water environment,<sup>1,4</sup> and the development of highly efficient arsenic adsorbents was the key for its success. In recent year, synthesized

metal oxides/hydroxides of nano-size had been explored as promising arsenic adsorbents due to their large surface areas and preferred surface properties.<sup>5,6</sup>

In natural water environment, most of arsenic contaminations exist as two major inorganic species, namely As(III) (arsenite) and As(V) (arsenate).<sup>7</sup> Due to its nonionic existence as H<sub>3</sub>AsO<sub>3</sub> in natural water, As(III) usually does not have high affinity to adsorbent surfaces compared with charged As(V),<sup>1,8</sup> while it is more toxic than As(V) in biological systems.<sup>9</sup> Thus, it usually required both a pre-treatment of oxidizing As(III) to As(V) and/or adjusting the pH value of water to weak acidic for its effective adsorption, and a post-treatment of adjusting the pH value of water back to the near neutral state.<sup>6,10,11</sup> So it would be desirable to develop novel arsenic nanoadsorbents with good As(III) adsorption capability under near neutral pH condition, which could largely simplify the treatment process and lower the treatment cost by removing the pre- and post-treatments.

In our recent theory study on the material criterion for the selection of highly efficient arsenic adsorbents,<sup>12</sup> a general material criterion was developed based on literature and our own work of creating arsenic adsorbents with strong arsenic adsorption in water.<sup>6,10,13-16</sup> It predicts that metal oxides/hydroxides may have good arsenic adsorption behavior if the metal element has the ionic potential (IP) from ~ 4 to ~ 7, which could provide the guidance for choosing proper arsenic adsorbent material candidate for study. Tin dioxide (SnO<sub>2</sub>) is an n-type, wide band gap semiconductor with interesting chemical, physical and mechanical properties, which is well known for applications in gas sensors, dye-based solar cells, transparent conducting electrodes, and catalyst supports etc.<sup>17-20</sup> The ionic potential of Sn<sup>4+</sup> is ~ 5.97, which meets the material criterion for potential strong arsenic adsorbent. To our best knowledge, however, no report was available in literature on the arsenic adsorption performance of SnO<sub>2</sub>.

<sup>a</sup>Shenyang National Laboratory for Materials Science, Institute of Metal Research, Chinese Academy of Sciences, Shenyang, Liaoning Province, 110016, P. R. China

<sup>b</sup>Zhangjiagang Green Tech Environmental Protection Equipment Co., LTD., Zhangjiagang, Jiangsu Province, 215625, P. R. China

<sup>c</sup>Department of Materials Science and Engineering, University of Illinois at Urbana-Champaign, Urbana, IL 61801, USA

<sup>†</sup>These authors contributed equally to this work.

\* Corresponding author: E-mail address: qili@imr.ac.cn.

Phone: +86-24-83978028, Fax: +86-24-23971215.

Postal address: 72 Wenhua Road, Shenyang, Liaoning Province, 110016, P. R. China.

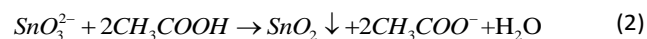
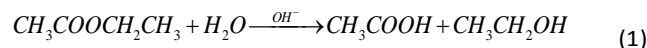
Electronic Supplementary Information (ESI) available: [details of any supplementary information available should be included here]. See DOI: 10.1039/x0xx00000x

Herein, we reported for the first time that SnO<sub>2</sub> could have a strong As(III) adsorption performance. A simple and cost-effective hydrolysis process was developed to synthesize SnO<sub>2</sub> nanospheres with the assistance of ethyl acetate under ambient conditions, which had a good dispersity, a narrow size distribution, a relatively large specific surface area, and a porous structure. Both the kinetics study and equilibrium adsorption isotherm study were conducted to examine the As(III) adsorption performance of these SnO<sub>2</sub> nanospheres, which demonstrated that they could effectively adsorb As(III) from water at near neutral pH environment with a relatively high Langmuir adsorption capacity of ~ 112.7 mg g<sup>-1</sup> at pH ~ 7. The As(III) adsorption mechanism on SnO<sub>2</sub> nanospheres was examined by both macroscopic and microscopic techniques, which demonstrated that it followed the inner-sphere complex mechanism. Even with exceptionally high concentrations of co-existing ions, these SnO<sub>2</sub> nanospheres could still effectively adsorb As(III) from water. A good regeneration capability was possessed by these SnO<sub>2</sub> nanospheres, which could reduce the operation cost significantly.

## Results and discussion

### Synthesis and Characterization of SnO<sub>2</sub> Nanospheres

In our synthesis process, the creation of SnO<sub>2</sub> nanospheres occurred spontaneously under ambient conditions in the EtOH and DI water mixture solution containing potassium stannate and ethyl acetate. In a basic environment induced by potassium stannate, hydrolysis reaction of ethyl acetate occurred easily, and formic acid was produced according to Eqn. (1). Subsequently, potassium stannate reacted with formic acid to form SnO<sub>2</sub> nanoparticles according to Eqn. (2).



To minimize the surface energy, these primary nanoparticles could gradually aggregate into large spherical particles to finally produce SnO<sub>2</sub> nanospheres. SnO<sub>2</sub> nanospheres could be produced in the ethanol and DI water mixture solution containing only potassium stannate as demonstrated by Archer et al. previously.<sup>20</sup> However, the yield was quite low without the addition of ethyl acetate (~ 47%) due to the slow hydrolysis reaction of potassium stannate along. In our synthesis process, formic acid was produced by the addition of ethyl acetate, which largely accelerated the hydrolysis reaction to produce SnO<sub>2</sub>. Thus, the SnO<sub>2</sub> yield was improved substantially in our synthesis process (~ 99%).

As shown in Fig. 1a, the X-ray diffraction pattern of as-synthesized SnO<sub>2</sub> nanospheres demonstrated that all XRD peaks could be indexed with the rutile primitive tetragonal structure of SnO<sub>2</sub> (JCPDS NO. 41-1445). The broadened peaks in their XRD pattern indicated that the products obtained were not well crystallized, which was due to their low reaction temperature at ~ 25 °C. Fig. 1b shows the FESEM image of SnO<sub>2</sub> nanospheres, which demonstrated clearly their spherical feature and good dispersity. The dynamic light scattering analysis result (inset in Fig. 1b) showed that these SnO<sub>2</sub> nanospheres had a relatively narrow size distribution. The average size of these SnO<sub>2</sub> nanospheres were ~ 170 nm, and their size varied mostly from ~ 80 nm to ~ 480 nm. Fig. 1c

shows the lower magnification TEM image of SnO<sub>2</sub> nanospheres, which also demonstrated clearly their spherical feature and good dispersity. It could be easily found that these SnO<sub>2</sub> nanospheres were composed of aggregated SnO<sub>2</sub> nanopatricsles with fine size. The higher magnification TEM image (inset in Fig. 1c) demonstrated that these SnO<sub>2</sub> nanopatricsles had the size of several nanometers, and they were highly porous. Fig. 1d shows the N<sub>2</sub> adsorption/desorption isotherms of these SnO<sub>2</sub> nanospheres, in which the adsorption followed the lower curve and the desorption followed the upper curve. Their BET specific surface area was calculated to be ~ 169.53 m<sup>2</sup> g<sup>-1</sup>. The insert in Fig. 1d shows the pore size distribution of SnO<sub>2</sub> nanospheres obtained by the Barrett-Joyner-Halenda (BJH) method from the desorption branch data, and the mesopore volume was determined at 0.11 cm<sup>3</sup> g<sup>-1</sup>. Thus, these SnO<sub>2</sub> nanospheres created by the hydrolysis process under ambient conditions had a relatively large surface area and porous structure, which was beneficial for their adsorption capability.

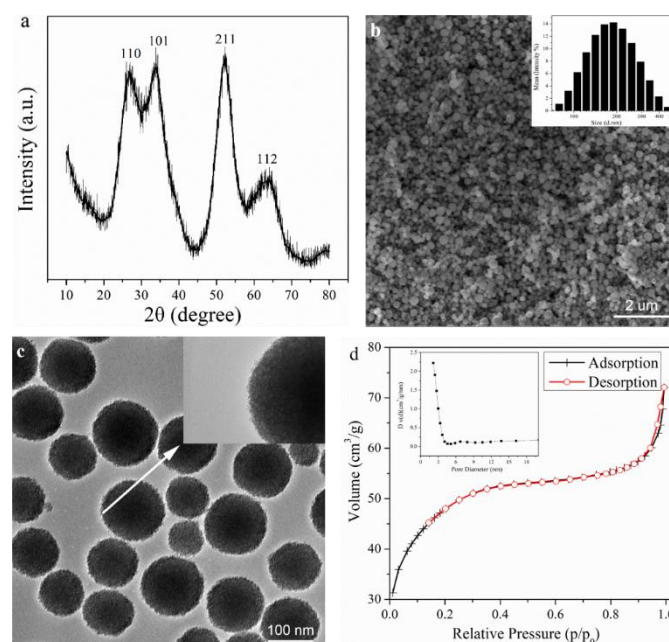


Fig. 1 (a) X-ray diffraction pattern, (b) FESEM image, (c) HRTEM image, and (d) N<sub>2</sub> adsorption/desorption isotherms of SnO<sub>2</sub> nanospheres, respectively (Note: Insert plots in Fig. 1b, 1c, and 1d show the size distribution, higher magnification TEM image, and the pore size distribution of SnO<sub>2</sub> nanospheres, respectively.).

### Kinetic Studies on Arsenite Adsorption by SnO<sub>2</sub> Nanospheres

Fig. 2 demonstrates the As(III) concentration decrease in lab-prepared water samples with the treatment time increase at different initial As(III) concentrations. With the SnO<sub>2</sub> nanosphere dosage increase, the As(III) removal rate increased and the final As(III) concentration in the treated water samples decreased. Fig. 2a shows the decrease of As(III) concentration with the increase of the treatment time when the initial As(III) concentration was ~ 85.7 μg L<sup>-1</sup> and the SnO<sub>2</sub> nanosphere dosage was 0.05 and 0.1 g L<sup>-1</sup>, respectively. After 100 min adsorption, As(III) concentration could be reduced to below the USEPA standard for arsenic in drinking water of 10 μg L<sup>-1</sup>.

when the SnO<sub>2</sub> nanosphere dosage was 0.1 g L<sup>-1</sup>. Fig. 2b shows the decrease of As(III) concentration with the increase of the treatment time when the initial As(III) concentration was ~ 1.32 mg L<sup>-1</sup> and the SnO<sub>2</sub> nanosphere dosage was 0.2 and 0.35 g L<sup>-1</sup>, respectively. Under such a high As(III) concentration, SnO<sub>2</sub> nanospheres still demonstrated a good As(III) adsorption performance. When the SnO<sub>2</sub> nanosphere dosage was just 0.2 g L<sup>-1</sup>, ~ 84% As(III) in the solution could be removed. Thus, a single adsorption step for the As(III) removal is practical with these SnO<sub>2</sub> nanospheres, which could eliminate oxidation and pH adjustment as the pre-treatment and another pH adjustment as the post-treatment.

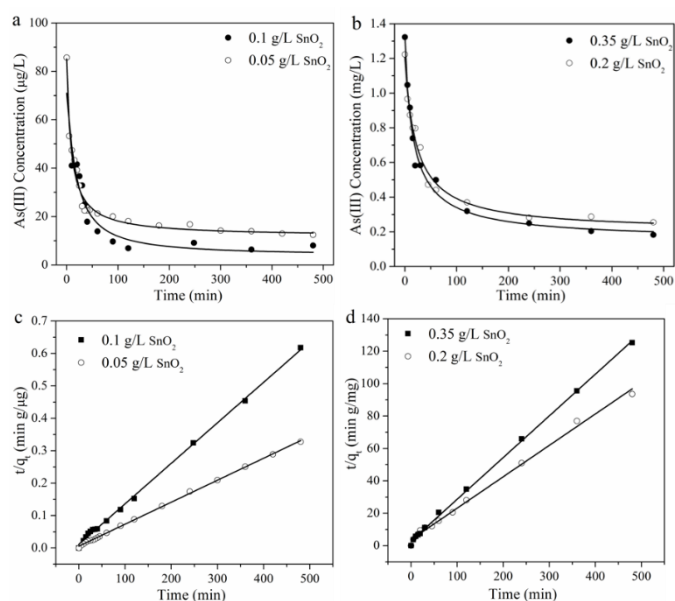


Fig. 2 Adsorption kinetics of As(III) on SnO<sub>2</sub> nanospheres with various material dosages and initial As(III) concentration of (a) ~ 85 µg L<sup>-1</sup> and (b) ~ 1.32 mg L<sup>-1</sup>. (c) and (d) The pseudo-second-order rate kinetic model fitting curves on data in Fig. 2a and 2b, respectively.

Fig. 2c and 2d show that the adsorption kinetic study results could be best fitted into a pseudo-second-order rate kinetic model for further understanding of the adsorption behavior. The integrated form of pseudo-second-order rate expression<sup>21,22</sup> is given in Eqn. (3), and its linear form is given in Eqn. (4):

$$q_t = \frac{K_{ad}q_e^2t}{1+q_eK_{ad}t} \quad (3)$$

$$\frac{t}{q_t} = \frac{1}{K_{ad}q_e^2} + \frac{t}{q_e} \quad (4)$$

where  $q_e$  is the equilibrium adsorption capacity (mg g<sup>-1</sup>),  $q_t$  is the amount (mg g<sup>-1</sup>) of As(III) adsorbed at time  $t$ , and  $K_{ad}$  is the rate constant of adsorption (g (mg•min)<sup>-1</sup>). Table 1 summarizes the kinetics parameters obtained in fitting the experimental data. The square of the correlation coefficient  $R$  ( $R^2$ ) quantified the applicability of the pseudo-second-order rate model. The closeness of  $R^2$  to 1 suggested that the kinetic experimental data could be well fitted by the pseudo-second-order rate kinetic model. Thus, a chemisorption<sup>6,16</sup> occurred between As(III) and SnO<sub>2</sub> nanospheres, which involved valency forces through sharing or exchange of electrons between SnO<sub>2</sub> nanospheres and As(III). This phenomenon had been found on

various As(III) adsorbents, whose As(III) adsorption was through the replacement of surface -OH by As(III).<sup>23,24</sup>

### Equilibrium Adsorption Isotherm Study of As(III) Adsorption by SnO<sub>2</sub> Nanospheres

The equilibrium adsorption isotherm study was conducted to investigate the As(III) adsorption capacity of SnO<sub>2</sub> nanospheres. As demonstrated in Fig. 3, the adsorption data was fitted with both Freundlich and Langmuir isotherms as given in Eqn. (5) and Eqn. (6), respectively:<sup>25</sup>

$$q_e = K_F C_e^{\frac{1}{n}} \quad (5)$$

$$q_e = \frac{q_{max}K_L C_e}{1+K_L C_e} \quad (6)$$

where  $q_e$  is the amount (mg g<sup>-1</sup>) of As(III) adsorbed at equilibrium,  $C_e$  is the equilibrium As(III) concentration (mg L<sup>-1</sup>) in water samples,  $K_F$  and  $n$  are the Freundlich constants,  $K_L$  is the Langmuir constant, and  $q_{max}$  is the Langmuir monolayer adsorption capacity. The fitting parameters were summarized in Table 2. It demonstrated clearly that the As(III) adsorption data could be better fitted with the Langmuir isotherm because its  $R^2$  was closer to 1 ( $R^2=0.991$ ) than that produced by the Freundlich isotherm ( $R^2=0.966$ ). The Langmuir adsorption capacity ( $q_{max}$ ) under the near neutral pH environment was determined at 112.7 mg g<sup>-1</sup>. Thus, SnO<sub>2</sub> nanospheres demonstrated a good As(III) adsorption performance among various As(III) nanoadsorbents.<sup>6,24,26-28</sup>

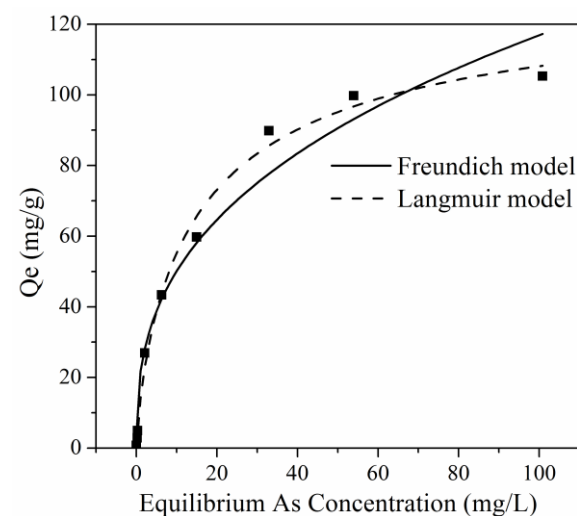


Fig. 3 The equilibrium adsorption isotherms of As(III) on SnO<sub>2</sub> nanospheres.

Table 1. Pseudo-second-order kinetics model fitting parameters for As(III) adsorption on SnO<sub>2</sub> nanospheres.

Initial As(III) concentration (mg L <sup>-1</sup> )	0.085		1.323	
SnO <sub>2</sub> loading (g L <sup>-1</sup> )	0.05	0.1	0.2	0.35
$q_e$ (mg g <sup>-1</sup> )	1.47	0.8	5.16	3.89
$K_{ad}$ (g mg <sup>-1</sup> min <sup>-1</sup> )	0.08	0.136	0.01	0.023
$R^2$	0.999	0.998	0.995	0.998

Table 2. Fitting parameters of Langmuir and Freundlich isotherms for As(III) adsorption on SnO<sub>2</sub> nanospheres.

Langmuir isotherm			Freundlich isotherm		
$q_{\max}$ (mg g <sup>-1</sup> )	$K_L$	$R^2$	n	$K_L$	$R^2$
112.7	0.128	0.991	1.68	10.43	0.966

### Electrophoretic Mobility Study of SnO<sub>2</sub> Nanospheres before and after Arsenite Adsorption

The macroscopic technique of electrophoretic mobility measurement was conducted to investigate the As(III) adsorption mechanism on SnO<sub>2</sub> nanospheres. The IEP of metal oxides is determined by protonation and deprotonation of surface hydroxyl groups. Fig. 4a shows the zeta potentials of SnO<sub>2</sub> nanospheres before and after As(III) adsorption. The isoelectric point (IEP) of SnO<sub>2</sub> nanospheres was determined at pH 3.8. At the near neutral pH environment, SnO<sub>2</sub> nanospheres were negatively charged, which indicated that the surface hydroxyl groups existed. The formation of outer-sphere surface complexes could not shift the IEP because no chemical reaction happens between the adsorbate and the adsorbent surface to change the surface charge, while only the formation of inner-sphere arsenic anionic charged surface complexes could cause the shift of IEP to a lower value.<sup>28-31</sup> After As(III) adsorption, the IEP of SnO<sub>2</sub> nanospheres decreased to ~ pH 3.1, which suggested that inner-sphere As(III) anionic charged surface complexes formed on SnO<sub>2</sub> nanospheres.

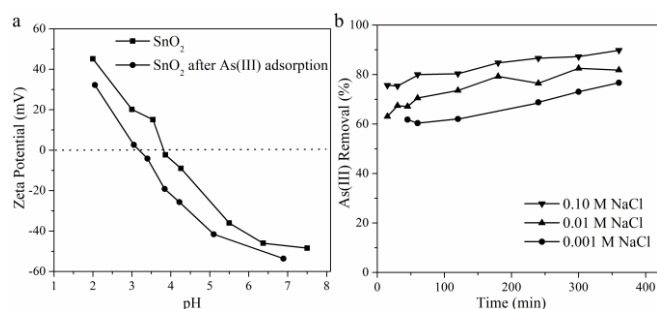


Fig. 4 (a) The zeta potentials of SnO<sub>2</sub> nanospheres before and after As(III) adsorption (0.1 g L<sup>-1</sup> SnO<sub>2</sub> nanosphere dosage and the initial As(III) concentration at ~ 100 mg L<sup>-1</sup>). (b) The As(III) removal efficiency with the increase of the solution ionic strength (0.1 g L<sup>-1</sup> SnO<sub>2</sub> nanosphere dosage and the initial As(III) concentration at 1 mg L<sup>-1</sup>).

### Ionic Strength Effect on Arsenite Adsorption by SnO<sub>2</sub> Nanospheres

Another macroscopic technique of evaluating the ionic strength effect on the As(III) adsorption behavior was also used to investigate the As(III) adsorption mechanism on SnO<sub>2</sub> nanospheres. The solution ionic strength was adjusted by the addition of NaCl with a series of concentrations from 0.001 M, 0.01 M to 0.1 M, while the initial As(III) concentration (1 ppm), the solution pH (~ 7) and the SnO<sub>2</sub> nanosphere dosage (0.1 g L<sup>-1</sup>) were kept the same. It had been reported that the adsorption of arsenic species would decrease with the increase of the solution ionic strength if arsenic species formed outer-sphere surface complexes, while it would not change or even increase with the solution ionic strength increase

when arsenic species formed inner-sphere surface complexes.<sup>32,33</sup> Fig. 4b shows that the removal efficiency of As(III) increased with the solution ionic strength increase at near neutral pH environment, which also suggested that the As(III) adsorptions on SnO<sub>2</sub> nanospheres followed the inner-sphere complex mechanism.

### FTIR Study of SnO<sub>2</sub> Nanospheres before and after Arsenite Adsorption

The microscopic technique of FTIR spectroscopy was further used to investigate the As(III) adsorption mechanism. Fig. 5 shows the FTIR spectrum variation of SnO<sub>2</sub> nanospheres before and after arsenite adsorption. The FTIR spectrum of SnO<sub>2</sub> nanospheres has strong hydroxyl stretching (3424 cm<sup>-1</sup>) and bending (1638 cm<sup>-1</sup>) vibrations of physically adsorbed H<sub>2</sub>O,<sup>34</sup> C=O stretching modes of adsorbed CO<sub>2</sub> (2352 cm<sup>-1</sup>) and bending vibrations (960 cm<sup>-1</sup>) of hydroxyl groups on metal oxides (Sn-OH).<sup>36</sup> After As(III) adsorption, the spectrum of Sn-OH bending vibrations (960 cm<sup>-1</sup>) decreased, which indicated that the replacement of -OH occurred during the arsenite adsorption. For As(III)/SnO<sub>2</sub>, a new peak at ~ 805 cm<sup>-1</sup> appeared after As(III) adsorption, which reflected the stretching vibration of uncomplexed As(III)-O bond.<sup>29</sup> The uncomplexed As(III)-O bond of dissolved arsenite species was determined at ~ 826 cm<sup>-1</sup> (see Fig. S1 in the Supplementary Information). The red shift of As(III)-O bond observed here could be attributed to the decrease of the strength of the uncomplexed As-O bond because of the formation of Sn-O-As(III) bond,<sup>29</sup> suggesting that inner-sphere complexes formed on As(III)/SnO<sub>2</sub>. The FTIR study results indicated that the substitution of surface -OH groups on SnO<sub>2</sub> nanospheres by As(III) species played the key role in their adsorption.

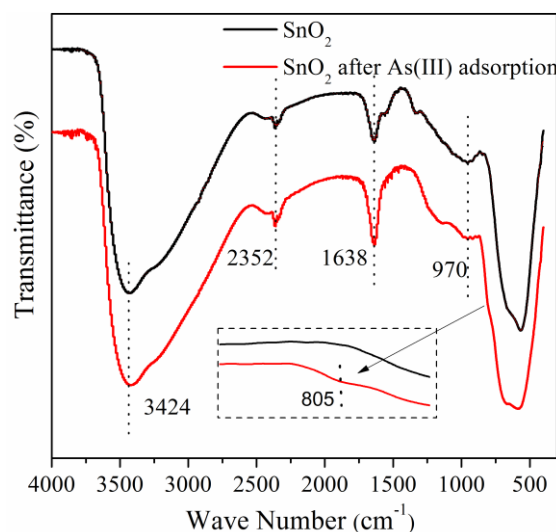


Fig. 5 FT-IR spectra of SnO<sub>2</sub> nanospheres before and after As(III) adsorption (0.1 g L<sup>-1</sup> SnO<sub>2</sub> nanosphere dosage and the initial As(III) concentration at ~ 100 mg L<sup>-1</sup>).

### Surface Chemical Compositions of SnO<sub>2</sub> Nanospheres before and after Arsenite Adsorption

To investigate the adsorption mechanism of As(III) on SnO<sub>2</sub> nanospheres, the chemical compositions and their status of SnO<sub>2</sub> nanospheres before and after As(III) adsorption were examined by the high-resolution X-ray photoelectron spectroscopy. Fig. 6a shows the Sn 3d spectra of SnO<sub>2</sub> nanospheres before and after As(III) adsorption. Both Sn 3d spectra demonstrated a spin-orbit doublet at ~ 486.2 eV (3d<sub>5/2</sub>) and ~ 495.3 eV (3d<sub>3/2</sub>), which suggested that

the chemical state of Sn in both samples was Sn(IV).<sup>37,38</sup> So the chemical state of Sn did not change in the As(III) adsorption process. A significant decrease of the intensities of Sn 3d peaks was observed after As(III) adsorption, indicating the occurrence of strong interactions between As(III) and SnO<sub>2</sub>.<sup>34</sup> Fig. 6b shows that As 3d spectra of SnO<sub>2</sub> nanospheres before and after As(III) adsorption. Before As(III) adsorption, no As 3d peak could be identified as expected. After As(III) adsorption, the binding energy of As 3d was at 44.8 eV,<sup>39</sup> indicating that As(III) species remained its chemical status during the As(III) adsorption process.

Fig. 6c and 6d show the O 1s spectra of SnO<sub>2</sub> nanospheres before and after As(III) adsorption, respectively. The peak position of the O 1s spectra shifted from 528.6 eV to 529.1 eV after the As(III) adsorption, which suggested that the chemical adsorption happened between SnO<sub>2</sub> and As(III).<sup>34</sup> The O 1s peak could be best fitted with three overlapped O 1s peaks of oxide oxygen (O<sup>2-</sup>), hydroxyl group (-OH), and adsorbed water (H<sub>2</sub>O).<sup>40</sup> Table 3 summarizes the fitting parameters of the data fitted by Lorentzian peak shape. Before the As(III) adsorption, the -OH percentage was ~ 53.69% of the total surface oxygen species, while it largely dropped to ~ 27.23% after the As(III) adsorption. The large decrease of hydroxyl group percentage could be attributed to the ligand exchange between surface -OH groups on SnO<sub>2</sub> nanospheres and As(III) species in water during the adsorption process. Thus, the XPS analysis suggested that the adsorption of As(III) onto the surface of SnO<sub>2</sub> nanospheres was a chemisorption process and the surface hydroxyl groups on SnO<sub>2</sub> nanospheres was the key contributor in this process.

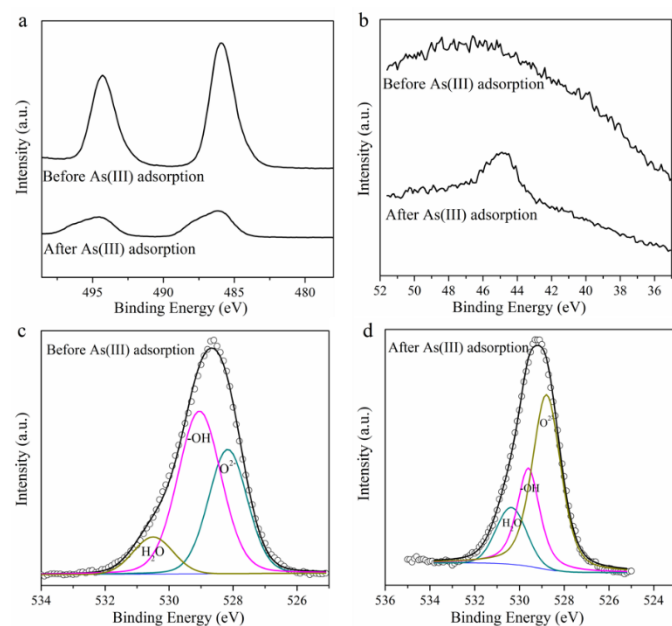


Fig. 6 XPS spectra on SnO<sub>2</sub> nanospheres before and after As(III) adsorption (0.1 g L<sup>-1</sup> SnO<sub>2</sub> nanosphere dosage and the initial As(III) concentration at ~ 100 mg L<sup>-1</sup>). (a) The surface Sn 3d spectrum, (b) The surface As 3d spectrum, (c) The surface O 1s spectrum before As(III) adsorption, and (d) The surface O 1s spectrum after As(III) adsorption.

Table 3. The Lorentzian peak shape fitting parameters for O 1s XPS peak of SnO<sub>2</sub> nanospheres before and after As(III) adsorption.

Samples	Peak	Position (ev)	Area	FWHM	Percent (%)
SnO <sub>2</sub>	H <sub>2</sub> O	530.5	18078.59	1.458	10.35
	-OH	529.05	93779.75	1.6	53.69
	O <sup>2-</sup>	528.164	62809.25	1.428	35.96
As(III)/SnO <sub>2</sub>	H <sub>2</sub> O	530.364	18167.39	1.60	16.33
	-OH	529.6	30289.66	1.20	27.23
	O <sup>2-</sup>	528.791	62791.63	1.51	56.44

### Competing Ion Effect on Arsenite Adsorption by SnO<sub>2</sub> Nanospheres

SO<sub>4</sub><sup>2-</sup>, HCO<sub>3</sub><sup>-</sup>, NO<sub>3</sub><sup>-</sup>, H<sub>2</sub>PO<sub>4</sub><sup>-</sup> and Ca<sup>2+</sup> were chosen as representatives in the competing ion effect examination because they usually co-exist with arsenic species in natural water and might affect the adsorption of arsenic species onto many adsorbents.<sup>41,42</sup> Fig. 7 shows the effects of these co-existing ions on As(III) adsorption by SnO<sub>2</sub> nanospheres at pH ~ 7. Two co-existing ion concentrations of 1 mM and 6.7 mM were chosen, for which the molar ratio of these co-existing ions to As(III) was set at 100:1 and 500:1, respectively. It demonstrated that SnO<sub>2</sub> nanospheres had a strong resistance to these co-existing ions even with such a high concentration. The presence of HCO<sub>3</sub><sup>-</sup>, NO<sub>3</sub><sup>-</sup> and Ca<sup>2+</sup> just showed a slight deterioration effect on As(III) adsorption by SnO<sub>2</sub> nanospheres. H<sub>2</sub>PO<sub>4</sub><sup>-</sup> is known for its strong hindrance effect to the adsorption of arsenic species.<sup>24,41</sup> Phosphorus and arsenic belong to the same element group (main group V), and phosphate could compete with arsenic species for active adsorption sites on adsorbents because its adsorption also followed the inner-sphere complexes mechanism and involved ligand exchange between phosphate in water and surface -OH groups on adsorbents.<sup>43-45</sup> Even with the presence of H<sub>2</sub>PO<sub>4</sub><sup>-</sup> at a high concentration of 500 times as that of As(III), the As(III) removal percentage by SnO<sub>2</sub> nanospheres could still be over 74.3% as that with no presence of co-existing H<sub>2</sub>PO<sub>4</sub><sup>-</sup>, which was much higher than that of various highly efficient arsenic nanoadsorbents.<sup>6,16,26</sup> Thus, these results demonstrated that SnO<sub>2</sub> nanospheres could effectively adsorb As(III) even with co-existing ions of exceptionally high concentrations.

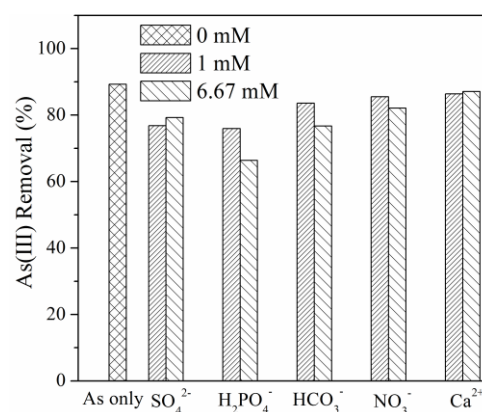


Fig. 7 Effects of co-existing ions on the As(III) adsorption on SnO<sub>2</sub> nanospheres at pH ~ 7 (0.1 g L<sup>-1</sup> SnO<sub>2</sub> nanosphere dosage and the initial As(III) concentration at ~ 1 mg L<sup>-1</sup>).

### Desorption of Arsenite from SnO<sub>2</sub> nanospheres

Fig. 8 shows the arsenite desorption percentage vs. NaOH solution concentrations, which demonstrated that the As(III) adsorbed on SnO<sub>2</sub> nanospheres could be easily desorbed by washing with NaOH solution. With the increase of the alkalinity of NaOH solution, the desorbed As(III) percentage increased gradually. When the NaOH concentration increased to 0.1 M, the As(III) desorption percentage could reach ~ 96.8%. When the NaOH concentration increased to 0.5 M, it further increased to ~ 99.2%. Thus, most As(III) adsorbed could be desorbed with the NaOH solution concentration at or over 0.1 M. It was much lower than the concentration of NaOH solution used for arsenic species desorption in some studies,<sup>23,27,46</sup> which could reduce the cost and ease the operation. After the desorption, recovered SnO<sub>2</sub> nanospheres could be reutilized, which could reduce the operation cost significantly.

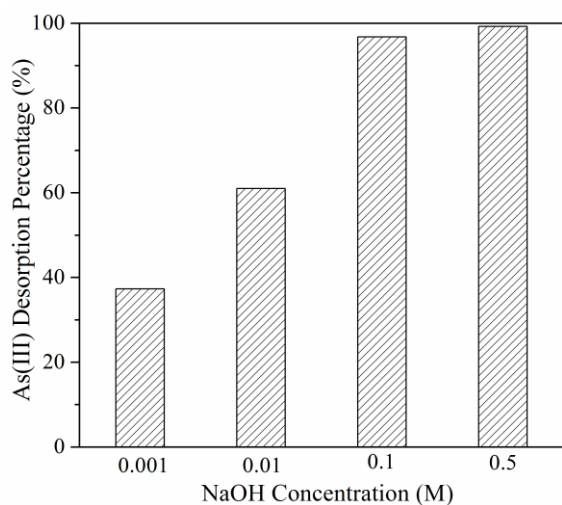


Fig. 8 Desorption of As(III) adsorbed on SnO<sub>2</sub> nanospheres by NaOH solutions with different concentrations from 0.001 M to 0.5M, respectively.

### Conclusions

In summary, SnO<sub>2</sub> nanospheres were successfully created by a simple and cost-effective hydrolysis process with the assistance of ethyl acetate under ambient conditions. These SnO<sub>2</sub> nanospheres had a good dispersity, a narrow size distribution, a relatively large specific surface area of ~ 169.53 m<sup>2</sup> g<sup>-1</sup>, and a porous structure. For the first time, it was demonstrated that these SnO<sub>2</sub> nanospheres could effectively adsorb As(III) from water at near neutral pH environment, and its Langmuir adsorption capacity at pH ~ 7 was determined at 112.7 mg g<sup>-1</sup>. At near neutral pH environment, the As(III) adsorption mechanism on SnO<sub>2</sub> nanospheres followed the inner-sphere complex model, and the surface hydroxyl groups on SnO<sub>2</sub> nanospheres played the key role in this process. SnO<sub>2</sub> nanospheres were found to be capable to effectively adsorb As(III) even with exceptionally high concentrations of co-existing ions. The adsorbed As(III) could be easily desorbed with NaOH solution washing and recovered SnO<sub>2</sub> nanospheres could be reutilized for the As(III) removal from water. Thus, SnO<sub>2</sub> nanospheres may have the potential to be a promising As(III) adsorbent for the As(III) removal from water without the pre-treatment of oxidation/pH adjustment and the post-treatment of another pH adjustment.

### Experimental

#### Chemicals and Materials

All the chemicals were purchased from Sinopharm Chemical Reagent Co., Ltd (Shanghai, P. R. China). They were of analytical reagent grade and were used without further purification. Potassium stannate trihydrate (K<sub>2</sub>SnO<sub>3</sub>•3H<sub>2</sub>O, 99.5%) was used as the Sn source in the synthesis process. Ethyl acetate (CH<sub>3</sub>COOC<sub>2</sub>H<sub>5</sub>, 99.5%) was used as the precipitation reagent. Deionized (DI) water and ethyl alcohol (EtOH, 99.7%) were used as solvents. Sodium arsenite (NaAsO<sub>2</sub>, 95%) was used to prepare As(III) stock solution. Sodium chloride (NaCl, 99.5%) was used for the ionic strength effect experiment. Sodium sulfate anhydrous (Na<sub>2</sub>SO<sub>4</sub>, 99%), sodium dihydrogen phosphate dehydrate (NaH<sub>2</sub>PO<sub>4</sub>•2H<sub>2</sub>O, 99%), sodium hydrogen carbonate (NaHCO<sub>3</sub>, 99.5%), sodium nitrate (NaNO<sub>3</sub>, 99%), and calcium chloride anhydrous (CaCl<sub>2</sub>, 96%) were used for the competing ion experiment. Sodium hydroxide (NaOH, 98%) were used for the arsenite desorption experiment.

#### Synthesis of SnO<sub>2</sub> Nanospheres

In a typical synthesis process, 40 mL of EtOH and 60 mL deionized (DI) water were added into a 250 mL beaker successively at 25 °C under vigorous stirring. Then, 0.8 mL CH<sub>3</sub>COOC<sub>2</sub>H<sub>5</sub> was added into the mixture solution. After 5 min more stirring, 0.3 g K<sub>2</sub>SnO<sub>3</sub>•3H<sub>2</sub>O powder was added into the solution within 5 min. The mixture solution pH gradually decreased to ~ 7 after being further stirred for ~ 110 min, suggesting that the hydrolytic reaction between CH<sub>3</sub>COOC<sub>2</sub>H<sub>5</sub> and K<sub>2</sub>SnO<sub>3</sub> was complete. Then, the white suspension was aged statically for 24 h at 25 °C. Finally, the suspension was centrifuged at 9900 rpm for 10 min, the obtained precipitates were rinsed with DI water and EtOH for several times to remove impurities, and dried at 40 °C overnight to obtain SnO<sub>2</sub> nanospheres.

#### Material Characterization

X-ray diffraction (XRD) pattern of the sample was obtained by a D/MAX-2004 X-ray powder diffractometer (Rigaku Corporation, Tokyo, Japan). Scanning electron microscopy (SEM) images were collected on a FEI Nova NanoSEM 450 microscope (FEI, Aht, The Netherlands). Transmission electron microscopy (TEM) images were collected on a JEOL 2100 TEM (JEOL Ltd., Tokyo, Japan) with an accelerating voltage at 200 kV, with point-to-point resolution of 0.28 nm. TEM samples were prepared by dispersing a thin film of SnO<sub>2</sub> nanospheres on Cu grid pre-coated with thin and flat carbon film. Nitrogen adsorption-desorption measurements were conducted with a Micrometrics ASAP 2020 system (Micrometrics TriStar II, USA). X-ray photoelectron spectroscopy (XPS) experiments were carried out on an ESCALAB 250 XPS system (Thermo Fisher Scientific Inc., Waltham, MA, USA) with an Al K anode (1486.6 eV photon energy, 0.05 eV photon energy resolution, 300 W). Attenuated total reflectance Fourier transform infrared spectra (ATR-FTIR) of SnO<sub>2</sub> nanospheres before and after As(III) adsorption were measured on a Nicolet 6700 FI-IR spectrometer with an attenuated total reflection attachment (Thermo Fisher Scientific Inc., Waltham, MA, USA). The zeta-potential of SnO<sub>2</sub> nanospheres at different pH was measured by a Malvern Nano ZS90 Zetasizer (Malvern Instruments Ltd., Malvern, Worcestershire, UK). The zeta-potential was determined by mixing 0.02 g SnO<sub>2</sub> nanospheres into 200 mL DI water with pH values adjusted between 3 and 10 by adding 0.1 M HCl or 0.1 M KOH.

### Arsenite Adsorption Experiment

The As(III) stock solution was prepared by dissolving proper amount of NaAsO<sub>2</sub> into DI water to reach 1.333 mM (~ 100 mg L<sup>-1</sup>) and stored in the dark in a refrigerator at 4 °C. In the adsorption kinetic study, the initial As(III) concentrations were adjusted to ~ 1.32 mg L<sup>-1</sup> and ~ 85.7 μg L<sup>-1</sup> by diluting the As(III) stock solution. The dosages of SnO<sub>2</sub> nanospheres were 0.05 g L<sup>-1</sup> and 0.1 g L<sup>-1</sup> for As(III) concentration at ~ 85.7 μg L<sup>-1</sup>, and 0.2 g L<sup>-1</sup> and 0.35 g L<sup>-1</sup> for As(III) concentration at ~ 1.32 mg L<sup>-1</sup>. In the equilibrium adsorption isotherm experiments, 0.1 g L<sup>-1</sup> SnO<sub>2</sub> nanospheres were added to As(III) solutions, and the As(III) concentrations varied from 0.5 mg L<sup>-1</sup> to 100 mg L<sup>-1</sup>.

During the adsorption experiments, 500 mL As(III) solution was first adjusted to pH 7 ± 0.5 with 0.1 M HCl and 0.1 M KOH. Then, SnO<sub>2</sub> nanospheres were added into the As(III) solution followed with 2 min ultrasonication for their dispersion. The suspension was sealed by plastic wrap immediately, and the adsorption experiments were all conducted at 25 °C with magnetic stirring at 500 rpm by an electric stirrer (JJ-1, Shanghai Pudong Physical Optical Instrument Factory Shanghai, P. R. China) to ensure a good contact between SnO<sub>2</sub> nanospheres with As(III). At appropriate time intervals, samples of the suspension were withdrawn and filtered by 0.22 μm syringe filter to obtain treated As(III) solutions for arsenic concentration measurement. To avoid the potential oxidation of As(III) to As(V), one drop of concentrated HCl was added into the clear solutions. The samples were analyzed by an atomic fluorescence spectrophotometer (AFS-9800, Beijing Ke Chuang Hai Guang Instrument Inc., Beijing, P. R. China) to determine the remaining As(III) concentrations. All experiments were in triplicate, and each reported result was the average of these three repeated tests.

To investigate the ionic strength effect on As(III) adsorption, the solution ionic strength was adjusted by the addition of 0.001 M, 0.01 M, and 0.1 M NaCl in As(III) solutions at near neutral pH (7±0.5). The dosage of SnO<sub>2</sub> nanospheres was 0.1 g L<sup>-1</sup> and the contact time was 24 h. To investigate the effect of competition ions on As(III) adsorption, SO<sub>4</sub><sup>2-</sup>, HCO<sub>3</sub><sup>-</sup>, NO<sub>3</sub><sup>-</sup>, H<sub>2</sub>PO<sub>4</sub><sup>-</sup> and Ca<sup>2+</sup> were chosen as co-existing ions. The concentration of each co-existing ion was 100 times and 500 times as that of As(III) (1 mg L<sup>-1</sup>) in the solution, respectively. The solution pH was adjusted to near neutral (7±0.5) before SnO<sub>2</sub> nanospheres were added (0.1 g L<sup>-1</sup>) and the total contact time was 24 h. For the As(III) desorption study, NaOH aqueous solution was chosen as the desorption solution, and the NaOH concentration effect on the As(III) desorption from SnO<sub>2</sub> nanospheres was examined with NaOH solutions of 0.001, 0.01, 0.1 and 0.5 M, respectively. After their equilibrium As(III) adsorption in water samples with initial As(III) concentration of ~ 4.2 ppm (equilibrium As(III) adsorption amount of ~ 30 mg g<sup>-1</sup>), 0.01 g SnO<sub>2</sub> nanospheres were dispersed into 100 mL NaOH solutions and the desorption time was 24 h.

### Acknowledgements

This study was supported by the Knowledge Innovation Program of Institute of Metal Research, Chinese Academy of Sciences (Grant No. YON5A111A1), the Youth Innovation Promotion Association, Chinese Academy of Sciences (Grant No. Y2N5711171), and the Basic Science Innovation Program of Shenyang National Laboratory for Materials Science (Grant No. Y4N56R1161).

### Notes and references

- 1 D. Mohan and C. U. Pittman Jr, *J. Hazard. Mater.*, 2007, **142**, 1-53.
- 2 T. S. Y. Choong, T. G. Chuah, Y. Robiah, F. L. Gregory Koay and I. Azni, *Desalination*, 2007, **217**, 139-166.
- 3 G. WHO, *Guidelines for drinking-water quality*, 2008.
- 4 M. Chiban, M. Zerbet, G. Carja and F. Sinan, *J. Environ. Chem. Ecotoxicol*, 2012, **4**, 91-102.
- 5 B. Chen, Z. Zhu, J. Ma, Y. Qiu and J. Chen, *J. Mater. Chem. A*, 2013, **1**, 11355-11367.
- 6 X.-Y. Yu, R.-X. Xu, C. Gao, T. Luo, Y. Jia, J.-H. Liu and X.-J. Huang, *ACS Appl. Mater. Interfaces*, 2012, **4**, 1954-1962.
- 7 P. L. Smedley and D. G. Kinniburgh, *Appl. Geochem.*, 2002, **17**, 517-568.
- 8 H. Lee and W. Choi, *Environ. Sci. Technol.*, 2002, **36**, 3872-3878.
- 9 C. K. Jain and I. Ali, *Water Res.*, 2000, **34**, 4304-4312.
- 10 G. Zhang, M. Sun, Y. Liu, X. Lang, L. Liu, H. Liu, J. Qu and J. Li, *ACS Appl. Mater. Interfaces*, 2015, **7**, 511-518.
- 11 I. A. Katsoyiannis, A. Voegelin, A. I. Zouboulis and S. J. Hug, *J. Hazard. Mater.*, 2015, **297**, 1-7.
- 12 R. Li, W. Yang, Y. Su, Q. Li, S. Gao and J. K. Shang, *J. Mater. Sci. Technol.*, 2014, **30**, 949-953.
- 13 L. S. Zhong, J. S. Hu, H. P. Liang, A. M. Cao, W. G. Song and L. J. Wan, *Adv. Mater.*, 2006, **18**, 2426-2431.
- 14 C. Hang, Q. Li, S. Gao and J. K. Shang, *Ind. Eng. Chem. Res.*, 2012, **51**, 353-361.
- 15 R. Li, Q. Li, S. Gao and J. K. Shang, *Chem. Eng. J.*, 2012, **185-186**, 127-135.
- 16 B. Chen, Z. Zhu, S. Liu, J. Hong, J. Ma, Y. Qiu and J. Chen, *ACS Appl. Mater. Interfaces*, 2014, **6**, 14016-14025.
- 17 Q.-H. Wu, J. Li and S.-G. Sun, *Current Nanoscience*, 2010, **6**, 525-538.
- 18 J. Liu, T. Luo, S. Mouli T, F. Meng, B. Sun, M. Li and J. Liu, *Chem. Commun.*, 2010, **46**, 472-474.
- 19 J. S. Chen and X. W. Lou, *Small*, 2013, **9**, 1877-1893.
- 20 X. W. Lou, Y. Wang, C. Yuan, J. Y. Lee and L. A. Archer, *Adv. Mater.*, 2006, **18**, 2325-2329.
- 21 Y. S. Ho and G. McKay, *Process Biochem.*, 1999, **34**, 451-465.
- 22 Y.-S. Ho, *J. Hazard. Mater.*, 2006, **136**, 681-689.
- 23 W. Tang, Y. Su, Q. Li, S. Gao and J. K. Shang, *Water Res.*, 2013, **47**, 3624-3634.
- 24 W. Tang, Q. Li, S. Gao and J. K. Shang, *J. Hazard. Mater.*, 2011, **192**, 131-138.
- 25 J. C. Y. Ng, W. H. Cheung and G. McKay, *Chemosphere*, 2003, **52**, 1021-1030.
- 26 M. Jian, B. Liu, G. Zhang, R. Liu and X. Zhang, *Colloid Surf. A*, 2015, **465**, 67-76.
- 27 H. Y. Niu, J. M. Wang, Y. L. Shi, Y. Q. Cai and F. S. Wei, *Microporous Mesoporous Mater.*, 2009, **122**, 28-35.

- 28 X. Sun, C. Hu and J. Qu, *Desalination and Water Treatment*, 2009, **8**, 139-145.
- 29 M. Pena, X. Meng, G. P. Korfiatis and C. Jing, *Environ. Sci. Technol.*, 2006, **40**, 1257-1262.
- 30 J. G. Catalano, C. Park, P. Fenter and Z. Zhang, *Geochim. Cosmochim. Acta*, 2008, **72**, 1986-2004.
- 31 M. Stachowicz, T. Hiemstra and W. H. van Riemsdijk, *J. Colloid Interface Sci.*, 2006, **302**, 62-75.
- 32 S. Goldberg and C. T. Johnston, *J. Colloid Interface Sci.*, 2001, **234**, 204-216.
- 33 M. B. McBride, *Clays Clay Miner.*, 1997, **45**, 598-608.
- 34 Y. Zhang, M. Yang, X.-M. Dou, H. He and D.-S. Wang, *Environ. Sci. Technol.*, 2005, **39**, 7246-7253.
- 35 S. Y. Ho, A. S. W. Wong and G. W. Ho, *Cryst. Growth Des.*, 2009, **9**, 732-736.
- 36 S. Fujihara, T. Maeda, H. Ohgi, E. Hosono, H. Imai and S.-H. Kim, *Langmuir*, 2004, **20**, 6476-6481.
- 37 Q. Ni, D. W. Kirk and S. J. Thorpe, *J. Electrochem. Soc.*, 2015, **162**, H40-H46.
- 38 M. Batzill and U. Diebold, *Prog. Surf. Sci.*, 2005, **79**, 47-154.
- 39 S. Ouvrard, P. de Donato, M. O. Simonnot, S. Begin, J. Ghanbaja, M. Alnot, Y. B. Duval, F. Lhote, O. Barres and M. Sardin, *Geochim. Cosmochim. Acta*, 2005, **69**, 2715-2724.
- 40 H. Cui, Q. Li, S. Gao and J. K. Shang, *J. Ind. Eng. Chem.*, 2012, **18**, 1418-1427.
- 41 M. Stachowicz, T. Hiemstra and W. H. van Riemsdijk, *J. Colloid Interface Sci.*, 2008, **320**, 400-414.
- 42 P. Smedley and D. G. Kinniburgh, *Arsenic in groundwater and the environment*, Springer, 2013.
- 43 Y. Su, H. Cui, Q. Li, S. Gao and J. K. Shang, *Water Res.*, 2013, **47**, 5018-5026.
- 44 J. Lǔ, H. Liu, R. Liu, X. Zhao, L. Sun and J. Qu, *Powder Technol.*, 2013, **233**, 146-154.
- 45 X. Yang, D. Wang, Z. Sun and H. Tang, *Colloid Surf. A*, 2007, **297**, 84-90.
- 46 G. Liu and H. Zhang, *The Adsorption of arsenic on magnetic iron-Manganese Oxide in Aqueous Medium*, Proceedings of the International Multi Conference of Engineers and Computer, 2008.